Steel and Composite Structures, *Vol. 18, No. 4 (2015) 873-887*
DOI: http://dx.doi.org/10.12989/scs.2015.18.4.873

Moment redistribution of continuous composite I-girder with high strength steel

Hyun Sung Joo [1], Jiho Moon [2], Ik-Hyun Sung [3] and Hak-Eun Lee [*1]

[1] *School of Civil, Environmental & Architectural Engineering, Korea University, 145 Anam-ro, Seongbuk-gu, Seoul 136-701, South Korea*
[2] *New Transportation Research Center, Korea Railroad Research Institute (KRRI), Uiwang-si, Gyeonggi-do, South Korea*
[3] *Department of Civil Engineering, Hanseo University, Chungcheongnam-do 356-706, South Korea*

(*Received August 20, 2013, Revised June 30, 2014, Accepted September 29, 2014*)

Abstract. The continuous composite I-girder should have a sufficient rotation capacity (or ductility) to redistribute the negative bending moment into an adjacent positive bending moment region. However, it is generally known that the ductility of the high strength steel is smaller than that of conventional steel, and application of high strength steel can cause ductility problems in a negative moment region of the I-girder. In this study, moment redistribution of the continuous composite I-girder with high strength steel was studied, where high strength steel with yield stress of 690 MPa was considered (the ultimate stress of the steel was 800 MPa). The available and required rotation capacity of the continuous composite I-girder with high strength steel was firstly derived based on the stress-strain curve of high strength steel and plastic analysis, respectively. A large scale test and a series of non-linear finite element analysis for the continuous composite I-girder with high strength steel were then conducted to examine the effectiveness of proposed models and to investigate the effect of high strength steel on the inelastic behavior of the negative bending moment region of the continuous composite I-girder with high strength steel. Finally, it can be found that the proposed equations provided good estimation of the requited and available rotation capacity of the continuous composite I-girder with high strength steel.

Keywords: rotation capacity; ductility; continuous I-girder; composite I-girder; high strength steel

1. Introduction

The high strength steel has been widely applied to a negative moment region of continuous composite I-girder and compressive flanges of the I-girder (Felkel *et al*. 2007). The continuous composite I-girder should have a sufficient rotation capacity (or ductility) to redistribute the negative bending moment into an adjacent positive bending moment region. The rotation capacity indicates the inelastic deformation capacity to maintain the strength without significant strength deterioration. When the rotation capacity in the negative moment region is not enough, plastic design based on the moment redistribution concept cannot be applied, and it leads to conservative design of the I-girder by ignoring the additional load carrying capacity of the girder system.

*Corresponding author, Professor, E-mail: helee@korea.ac.kr

http://www.techno-press.org/?journal=scs&subpage=8 ISSN: 1229-9367 (Print), 1598-6233 (Online)

Lay and Galambos (1967) proposed an equation to estimate the rotation capacity of beams under moment gradient, considering lateral-torsional buckling and local buckling of the flange and webs. Kemp and Dekker (1991) suggested an equation to predict the rotation capacity of an I-girder in the negative moment region. Kemp (1996) extended his previous research (Kemp and Dekker 1991) to propose the simple equation for predicting the rotation capacity of the non-composite and composite beam. Also, rotation capacity in the negative moment region of an I-girder has been studied by several researchers up to recently (Barth *et al*. 2000, Kemp and Nethercot 2001, Guzelbey *et al*. 2006, Chen and Jia 2008, Cevik 2007, 2011).

AASHTO LRFD Appendix B6 (2007) provides an alternative plastic design method for the continuous composite I-girder, considering the moment redistribution concept. However, AASHTO LRFD Appendix B6 (2007) specifies the yield stress limit of 485 MPa to apply this design concept. Recently, the yield stress of the steel has been increasing dramatically. In South Korea, high strength structural steel named HSB 800 was developed, where yield and ultimate stress were 690 MPa and 800 MPa, respectively. It is doubtful that results of previous researchers and AASHTO LRFD Appendix B6 (2007) are still applicable for this high strength steel, since the material properties of the high strength steel is quite different from that of conventional structural steel. The major difference is that the plastic plateau is negligibly small, and strain hardening appears immediately after yielding. In addition, several researchers pointed out that applications of high strength steel could cause ductility problems for I-girder bridges (Felkel *et al*. 2007, Ricles *et al*. 1998, Sause and Fahnestock. 2001, Green *et al*. 2002, Barth *et al*. 2007, Earls and Shah. 2002, Joo *et al*. 2013).

In this study, the moment redistribution of the continuous composite I-girder with high strength steel (HSB 800) was studied. The available and required rotation capacity of the continuous composite I-girder with high strength steel were proposed based on the stress-strain curve of high strength steel and plastic analysis, respectively. A large scale test and non-linear finite element analysis for the continuous composite I-girder with high strength steel was then conducted to examine the effectiveness of proposed models.

2. Available and required rotation capacity

The plastic design method based on the moment redistribution concept can be applied to the continuous composite I-girder when the girder has a sufficient rotation capacity. To provide the sufficient rotation capacity, the rotation capacity of the section must be larger than the required rotation capacity of the continuous composite I-girder, where the rotation capacity of the section is defined as the available rotation capacity, θ_a, and the required rotation capacity, θ_r, represents the inelastic deformation that is required to ensure full plastic action of the continuous composite I-girder. It should be noted that θ_a is the sectional properties, while θ_r varies depending on the many parameters of the girder system such as loading cases, the span ratio of continuous I-girder, and plastic moment and stiffness ratio between positive and negative moment region. The theoretical derivations of θ_a and θ_r for the continuous composite I-girder with high strength steel were discussed in this section.

2.1 Available rotation capacity

Fig. 1 shows the typical applied moment-rotation relationship of the negative bending moment region of the continuous composite I-girder. In Fig. 1, θ_p and θ_u are the rotations of the girder

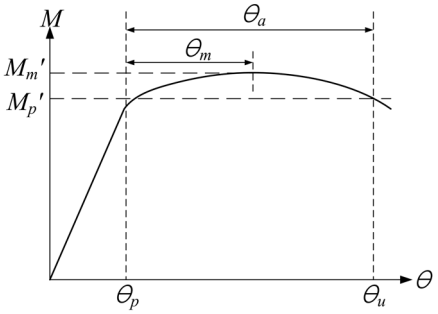

Fig. 1 Typical M-θ relationship

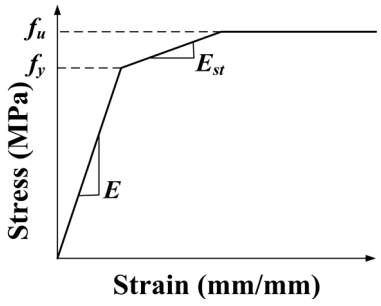

Fig. 2 Typical stress-strain curve for high strength steel.

corresponding to plastic moment of the section in the negative bending moment region, M_p', (where θ_u is larger than θ_p) and M_m' is the maximum moment resistance of the section in the negative bending moment region. Then, the available rotation capacity θ_a is defined as θ_u - θ_p. It is noted that plastic moment of the section in negative (and positive) bending was obtained from general plastic stress distribution method (PSDM). In PSDM, the tensile stress of the concrete is assumed as zero, and the maximum compression of the concrete is limited to $0.85f_c'$. Further, at the ultimate stage, it is assumed that the steel and the reinforcement are fully yielded.

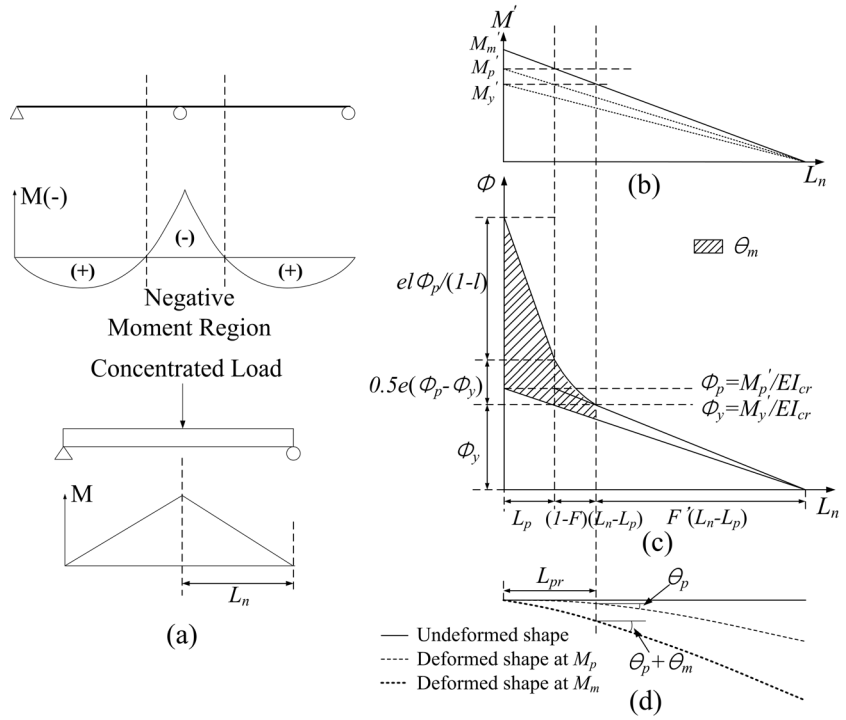

Fig. 3 Derivation of the available rotation capacity of the composite continuous I-girder: (a) negative bending moment region and simple beam analogy; (b) moment diagram in L_n; (c) curvature distribution; and (d) deformed shapes

Joo *et al*. (2013) proposed an equation to estimate the available rotation capacity of the non-composite I-girder with high strength steel, based on a material property of high strength steel shown in Fig. 2. In this study, their approach was modified to estimate θ_a of the continuous composite I-girder with high strength steel. From the Fig. 2, for high strength steel, it can be seen that the plastic plateau is negligibly small, and strain hardening appears immediately after yielding up to ultimate stress of the steel.

Fig. 3 shows the schematic view of the derivation of the available rotation capacity of the composite continuous I-girder. Fig. 3(a) represents the negative bending moment region of the two-span composite continuous I-girder and its simple beam analogy. Generally, negative bending moment region is modeled by using the simple beam under central concentrated load, since the shape of the negative bending moment of such beam is similar with that of negative bending moment region of the continuous I-girder. Figs. 3(b), (c) and (d) show the bending moment diagram, curvature distribution, and deformed shape of the girder in negative bending moment region of the continuous composite I-girder, respectively. In Fig. 3, L_n represents the length of the negative moment region. L_{pr} denotes the yield length, where it is defined as the distance from the internal support to the extreme fiber that is yielded. L_p is the plastic length, where L_p can be obtained from the distance from the internal support to the point of the cross-section that is fully yielded. θ_p is the rotation corresponding to elastic limit. θ_m is the rotation corresponding to M_m' (Refer Fig. 1). Based on the stress-strain curve shown in Fig. 2, the curvature distribution can be obtained as Fig. 3(c). Then, the shade area in Fig. 3(c) represents the plastic rotation corresponding to the maximum negative moment resistance of the section, M_m, at the point of L_{pr}, and it is defined as θ_m. θ_m is given by

$$\theta_m = \frac{M'_p L_n}{4(1-l)EI_{cr}}\left[(e-2)(1-F')^2 + 2\left(F'\left(e-eF'-2+F'\right)+1\right)l + \left(e+F'^2(e+2)\right)l^2 + 2F'^2 l^3\right] \quad (1)$$

In Eq. (1), EI_{cr} is the flexural stiffness of negative moment region, and EI_{cr} can be simply obtained by neglecting the contribution of the concrete on the flexural stiffness. e is defined as E/E_{st}, where E_{st} is the strain hardening modulus. F' is M_y'/M_p', where M_y' is the yielding moment of negative moment region. m is defined as M_m'/M_p'. l is L_p/L_n, and l is equal to 1-1/m from the geometric relation. The plastic length L_p must be determined first to use Eq. (1). Kemp and Dekker (1991) proposed L_p considering the inelastic lateral-torsional buckling and local buckling of the flange and the web. In this study, L_p proposed by Kemp and Dekker (1991) was used. The details for determination of L_p can be found in the research of Kemp and Dekker (1991).

Usually, θ_a is assumed as twice of θ_m. However, Joo *et al*. (2013) reported that this relationship is not proper for I-girder with high strength steel. They suggested the relationship between θ_m and θ_a based on the results of extensive parametric study, and their result was adopted to calculate θ_a in this study. The relationship between θ_m and θ_a proposed by Joo *et al*. (2013) is given by

$$\theta_a = 1.8809\theta_m - 0.0044 \quad (2)$$

Finally, based on the Eqs. (1) and (2), θ_a for the continuous composite I-girder with high strength steel can be obtained.

Joo *et al*. (2013) reported that the rotation capacity of an I-girder with high strength steel is usually smaller than that of an I-girder with normal strength steel, since the modulus of elasticity is not changed, while the elastic deformation prior to the plastic moment proportionally increases

with increasing yield stress. They suggested the optimum bracing point to maximize the rotation capacity of the girder. They found that out-of-plane deformation can be effectively restrained when the length of the yielded region is close to the unbraced length, and it leads to increased rotation capacity of the girder. Thus, to increase the rotation capacity of the girder, L_{pr} should be equal to the unbraced length L_b. The normalized unbraced length factor α was suggested as

$$\alpha = \frac{L_n - L_b}{L_n}. \tag{3}$$

From Eq. (3), it can be seen that the bracing is installed in mid-point of the length of the negative moment region, L_n, when α is equal to 0.5. From the results of Joo *et al*. (2013), the optimum bracing point, α_o, that maximize the rotation capacity of the girder can be obtained as

$$\alpha_o = \frac{M'_y}{M'_{m(0.5)}} \tag{4}$$

where $M'_{m(0.5)}$ and M'_y are the maximum moment resistance when α is equal to 0.5 and yield moment of the section in negative bending moment region, respectively.

2.2 Required rotation capacity and failure load

The required rotation capacity represents the inelastic deformation that is necessary to ensure full plastic action of the continuous composite I-girder. The required rotation capacity of the negative moment region of the composite continuous I-girder depends on the many parameters. In this section, the concept of the required rotation capacity of general multi-span continuous composite I-girder was discussed first. Then, an example for required rotation capacity and failure load of the two-span continuous I-girder with uniform section and concentrated loads was presented.

To quantify the failure load of the continuous I-girder, it is assumed that the flexural behavior of composite I-girder follows a bilinear elasto perfectly plastic moment-curvature response. Thus, the maximum flexural capacity of the section is limited to the plastic moment of the section. This assumption is reasonable to predict the failure load, even if the maximum moment capacity of the section is equal to M_m (Refer Fig. 1), since the difference between M_p and M_m is generally not large and it gives a conservative estimation of the failure load of the continuous composite I-girder, remaining the simplicity of the calculation. However, it must be noted that this assumption give an un-conservative prediction of the required rotation capacity, since the plastic deformation continuously increase until the failure of whole girder system, and achieving M_p of the section doesn't means the failure of the whole girder system. Thus, the collapse of the girder system must be considered to evaluate the required rotation capacity.

Fig. 4 shows the multi-span continuous composite I-girder under arbitrary load and equivalent single span. The negative bending moments are developed at internal support *A* and *B*, as shown in Fig. 5. In the negative bending moment region, the cracks in concrete slab are developed in early loading stages. Thus, flexural stiffness of the section in negative bending moment region, EI_{cr}, can be obtained by neglecting the contribution of the concrete slab on the flexural stiffness. In Fig. 5, EI_{un} represent the effective flexural stiffness of the section under positive bending moment. In this study, EI_{un} proposed by Nie and Cai (2003) was used throughout this study, and it is given by

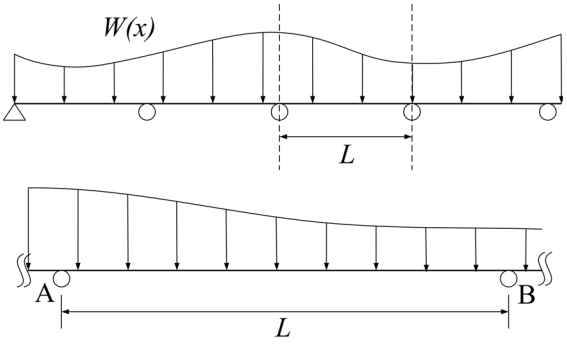

Fig. 4 Multi-span continuous composite girder and equivalent single span

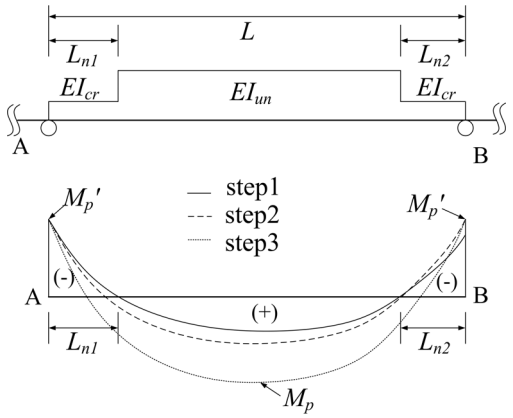

Fig. 5 Flexural stiffness and moment diagram of equivalent single span

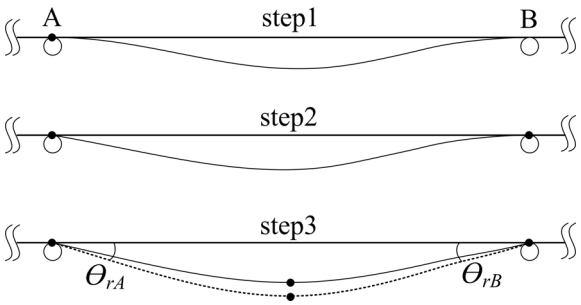

Fig. 6 Plastic hinge propagation with increasing the applied moment

$$EI_{un} = \frac{EI}{1+\xi} \tag{5}$$

where EI is the flexural stiffness of the gross section, and ξ is the factor to take account of the effect of shear slip considering the stiffness of the stud. In Fig. 5, L_{n1} and L_{n2} represents the length of negative bending moment region near internal support A and B, respectively (Refer Fig. 5).

Let's assume that the rotation capacity of the point A and B are sufficient, and the negative bending moment at point A reaches to M_p' first (Refer Step 1 in Figs. 5 and 6) where M_p' represent the plastic moment of the section in negative moment region while M_p in Fig. 5 denotes the plastic moment of the section in positive moment region. Even if the point A reaches to M_p', the additional loading can be applied, since the continuous composite I-girder has several redundant. With increasing the applied loading, the point B may reach to M_p', while the moment in point A remains M_p' (Refer, step 2 in Figs. 5 and 6). Then, the load gradually increases until the plastic hinge is formed at the positive bending moment region (Refer solid line in Step 3 in Fig. 5 and 6). Finally, the deformation increase until the girder collapse. (Refer dashed line in Step 3 in Fig. 5 and 6). At this ultimate state, the rotation at point A and B (θ_{rA} and θ_{rB}) are defined as the required rotation capacity at point A and B, respectively.

For the two-span continuous composite I-girders with uniform cross section and concentrated loads shown in Fig. 7, the failure load and required rotation capacity were evaluated as an example. From the Fig. 7, it can be found that the maximum negative bending moment occurs at point *C*. Thus, the first plastic hinge will be formed at point *C* when the section moment at point *C* reaches to M_p'. The applied load corresponding to this state was defied as P_h in this study. P_h is affected by the flexural stiffness ratio between positive and negative bending moment region, EI_{cr}/EI_{un}, since the bending moment diagram of the girder vary depending on EI_{cr}/EI_{un} and the length of the negative bending moment region, L_n, is also affected by EI_{cr}/EI_{un}. Generally, P_h can be obtained as following form

$$P_h = a_1 \frac{M'_p}{L} \tag{6}$$

In Eq. (6), a_1 represent the coefficient that varies depending on EI_{cr}/EI_{un}. In this study, a_1 was derived as a function of EI_{cr}/EI_{un}, and it is plotted in Fig. 8. By using the chart shown in Fig. 8, a_1 can be easily obtained.

If the rotation capacity of the composite I-girder in negative bending moment is not sufficient, the failure load is equal to Eq. (6), since the moment redistribution cannot be expected due to brittle behavior in negative bending moment region. On the other hand, if the rotation capacity is

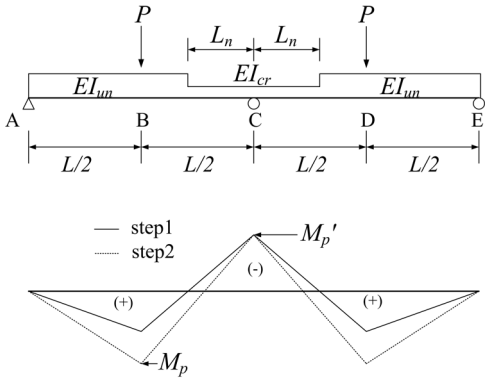

Fig. 7 Two-span continuous composite I-girder with uniform section and concentrated loads

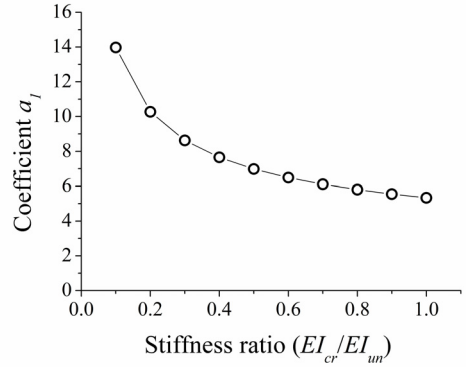

Fig. 8 Variation of a_1 in EI_{cr}/EI_{un}

sufficient in negative bending moment region (Point *C*), the additional load can be applied to the girder up to the failure of the girder. After forming the plastic hinge at point *C*, *AC* and *CE* span can be assumed as simply supported beam for the additional load, ΔP. Then, the magnitude of ΔP can be obtained by assuming the Point *B* and *D* reaches to plastic moment M_p. Finally, the failure load P_u of the composite I-girder shown in Fig. 7 can be calculated by summing P_h in Eq (6) and ΔP. Thus, P_u can be obtained as

$$P_u = \frac{2M_p(2+\mu)}{L}. \tag{7}$$

In Eq. (7), μ represents the plastic moment ratio between the negative and positive bending moment region, and it is defined as M_p'/M_p. It should be noted that P_u is only possible when the available rotation capacity of the section is larger than the required rotation capacity of the girder.

The required rotation capacity divides into two parts. The first one is the rotation that is needed to develop the plastic moment in positive bending moment region after forming the plastic hinge at point *C*. It should be noted that the rotation at point *C* is equal to zero when the section moment is less than M_p'. Thus, the first part of the required rotation is the same with the rotation that is generated by ΔP. Then, the rotation is continuously increases up to the failure of the positive section. This additional rotation is a second component of the required rotation capacity. In this study, it is assumed that the failure of the girder in positive bending moment region occurs when the concrete extreme fiber strain is equal to 0.003. Fig. 9 shows the curvature distribution of point *B* and *D* when the concrete extreme fiber strain is equal to 0.003. Thus, the second part of the required rotation capacity at point *C* can be obtained by calculating the dashed area in Fig. 9, since the slope at point *B* and *D* is equal to zero. In Fig. 9, D_p is the distance from the top of the concrete slab to the neutral axis of the composite section at the plastic moment, and *F* is M_y/M_p (where M_y is the yielding moment of positive moment region).

Finally, the required rotation capacity, θ_r, can be expressed as

$$\theta_r = \frac{LM_p'(6-5\mu)}{16\mu EI} + \left(\frac{0.003}{D_p} - \frac{M_p}{EI}\right)\frac{(1-F)L}{4(1+\mu)} \tag{8}$$

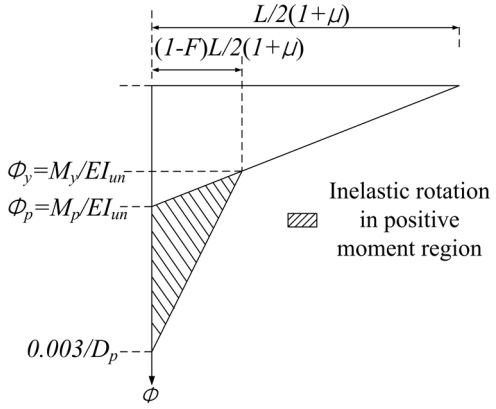

Fig. 9 Curvature distribution in positive moment region at ultimate state (Point *B* and *D*)

In Eq. (8), the first and second term represent the rotation that is generated by ΔP and additional rotation that is calculated based on the curvature diagram in Fig. 9, respectively.

3. Test specimen and test setup

3.1 Test specimen and test setup

An experimental study was conducted to examine the validation of proposed equations for available and required rotation capacity of the continuous composite I-girder with high strength steel. A large scale two-span continuous composite I-girder with high strength steel was constructed for the test, as shown in Fig. 10.

The length of the girder was 11,600 mm, the depth of steel I-girder, d, was 340 mm, the thickness of the web, t_w, was 15 mm, the width of the flange, b_f, was 120 mm, and the thickness of the flange, t_f, was 20 mm. The specimen was fabricated with HSB800 steel. From the material test, the yield and ultimate stress of the flange were 823.1 MPa and 920.8 MPa, respectively, and the yield and ultimate stress of the web were 725.3 MPa and 867.3 MPa, respectively. The two main I-girders were connected by cross beams, and the distance from the center to center of the two main I-girders was 800 mm. In the case of the cross beam, the thickness of the web and flange were both 10 mm. In order to increase the rotation capacity of the test specimen, the bracings near the internal supports were un-equally installed. From Eq. (4), the optimum bracing point was founded at $\alpha_o = 0.771$, and $\alpha = 0.756$ was used for the test. The depth of concrete slab was 120 mm, and the width of concrete slab was 1,200 mm. The compressive strength of concrete slab was 32 MPa from the material test. The area and yield stress of the reinforcing bar were 549.8 mm^2 and 400 MPa, respectively. Concentrated loads were applied at the 1/4 and 3/4 of the span.

Based on the geometry and material properties of the test specimen, it was found that the plastic moment in positive bending moment region, M_p, and plastic moment in negative bending

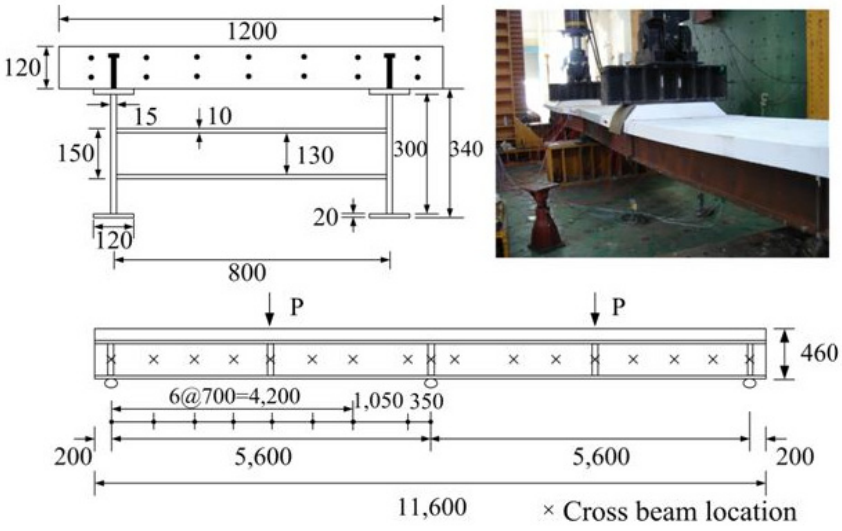

Fig. 10 Schematic view of test setup and dimensions of test specimen

moment region, M_p', were 1266.1 kN·m and 921.8 kN·m, respectively. θ_r and θ_a were 0.02893 rad and 0.05138 rad, respectively. Thus, full plastic action was expected for the test specimen, since θ_a was larger than θ_r. It is also noted that the number of shear connector in the test specimen were selected to ensure the full shear connection. As a result, the plastic moment of the section can be simply obtained by using the plastic stress distribution method, and it is assumed that the concrete slab and steel girder is perfectly bonded each other.

3.2 Test results and comparisons

Figs. 11(a) and (b) show the comparison of the applied load-displacement relationship and the applied load-curvature relationship, respectively. The displacement shown in x axis in Fig. 11(a) was obtained by averaging the displacement at 1/4 and 3/4 of the span. P_h and P_u shown in Figs. 11(a) and (b) were obtained from the proposed equation shown in section 2.2. P_h and P_u were 1,904.7 kN and 2,399 kN, respectively, based on the proposed Eqs. (6)-(7). From the test results, the discrepancy of P_u between the proposed equation and test was approximately 2.62 %, and test results agree well with the proposed equation. From the Fig. 11(b), it can be found that the stiffness of the applied load-curvature curve in negative bending moment region (Solid line in Fig. 11(b)) was considerably reduced after passing P_h, while the stiffness of the applied load-curvature curve in positive bending moment region significantly reduced near P_u. This imply that the plastic hinge formed approximately at P_h in negative bending moment region, and the girder collapsed by the failure of the positive bending moment region. Thus, it also support that the proposed equations provide the reasonable prediction of P_h and P_u.

The curvature of the negative bending moment region of the test specimen was calculated from the strain data. From Fig. 12, it can be seen that L_{pr} obtained from the theory was almost identical with that from the test. Further, the shade area in Fig. 12 represents the rotation that is required to develop P_u of the test specimen, and it was 0.02725. This value was similar with the required rotation capacity obtained from proposed equation in section 2.2 (θ_r from Eq. (8) was 0.02893). Thus, it can be conclude that the proposed equation for θ_r compared well with the test results.

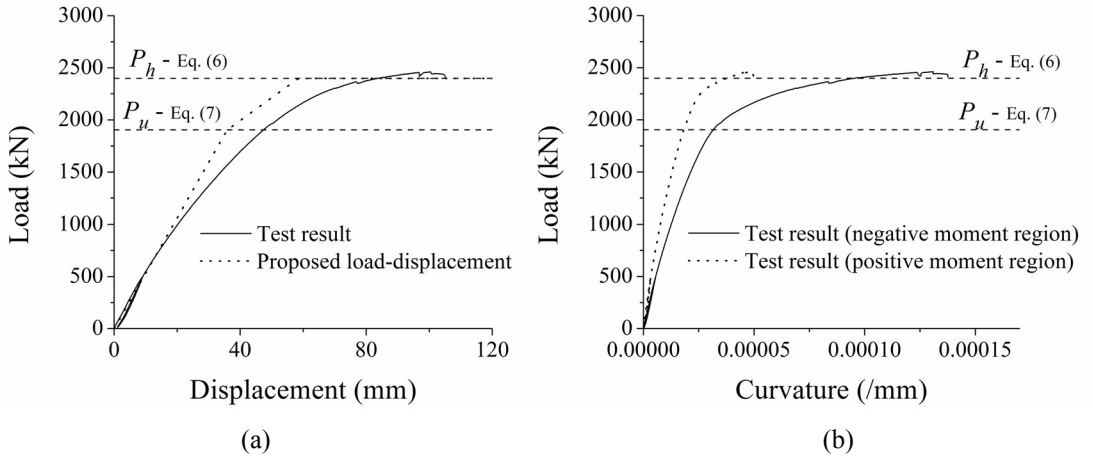

Fig. 11 Comparison of test results with proposed equation: (a) applied load vs. displacement; and (b) applied load vs. curvature

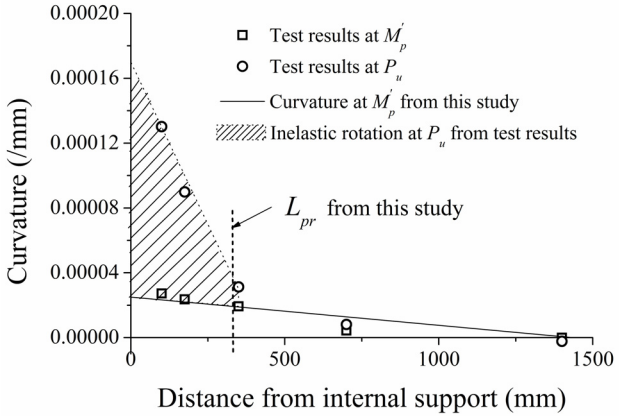

Fig. 12 Comparison of curvature distribution of the negative bending moment region

4. Additional verification of available rotation capacity

4.1 Finite element model overview

From the test, the failure load and the required rotation of the test specimen well with proposed equations. Further, it can be found that the available rotation capacity of the test specimen was larger than the required rotation capacity, since the moment redistribution was observed and the girder collapsed by the failure of the positive bending moment region. However, it is hard to quantify the available rotation capacity of the negative bending moment region from the test. Thus, to verify the proposed available rotation capacity of the negative moment region of the continuous composite I-girder with high strength steel, additional verification was conducted the based on the non-linear finite element analysis.

Only negative bending moment region was modeled in this study to evaluate the available rotation capacity, as shown in Fig. 13. The bottom of mid-span of the girder was restrained in

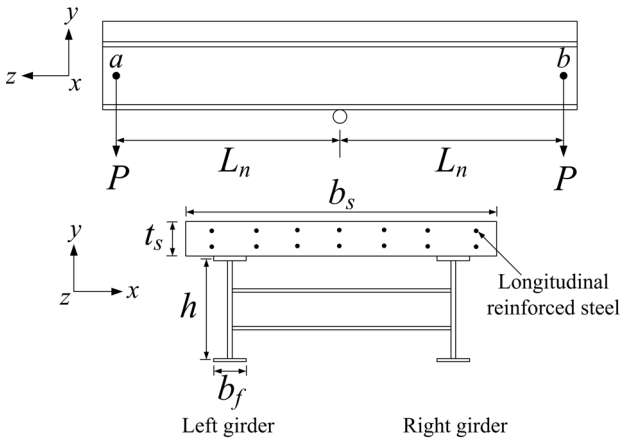

Fig. 13 Analysis model and the cross section of the composite I-girder

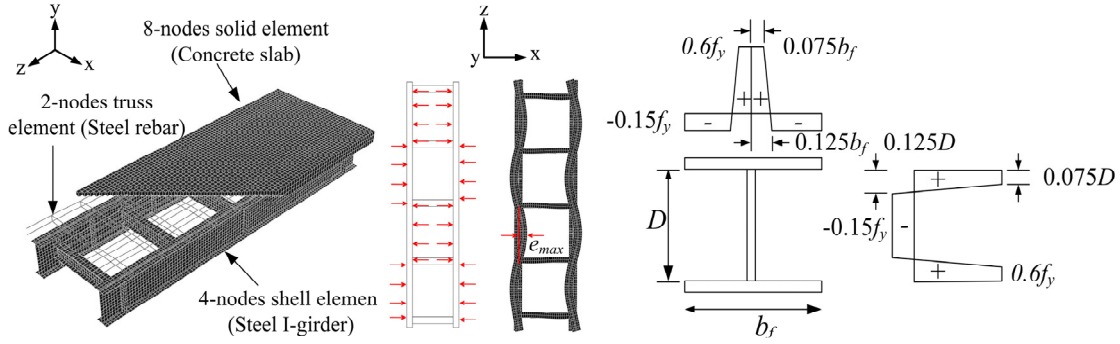

Fig. 14 Analysis model: (a) finite element model; (b) initial imperfection; and (c) residual stresses

vertical direction (y direction). The point a of the right and left girder was constrained in longitudinal direction (z direction), and point a and b of the right girder was restrained in out-of-plane direction (x direction).

The structural analysis program ABAQUS (2010) was used for the analysis. Fig. 14(a) shows the finite element model used in this study. 8-node solid element with reduced integration (C3D8R) and 4-node shell element with reduced integration (S4R) were used to model the concrete slab and steel I-girder, respectively. 2-node truss element (T3D2) was used to simulate the longitudinal and transverse reinforced rebar. To invoke the lateral-torsional buckling of the girder, the initial imperfection shown in Fig. 14(b) was introduced, where the maximum magnitude of the initial imperfection, e_{max}, was taken as 1/2,000 of the unbraced length of the compression flange. Residual stress is also an important parameter that affects the inelastic behavior of the girder. For a welded I-girder section with HSB800, Kang *et al*. (2011) proposed the distribution of the residual stress of HSB800, as shown in Fig. 14(c). It can be seen that the maximum tensile and compression residual stress are $0.6f_y$ and $0.15f_y$, respectively, and these are somewhat lower than those of normal steel. In this study, the distribution of the residual stress shown in Fig. 14(c) was used.

The compressive strength of the concrete used for the analysis was assumed as 32 MPa. For the compression part, the uniaxial stress-strain relationship of the concrete was assumed to follow simple parabolic curve. In the case of the uniaxial tensile behavior of the concrete, stress-strain curve proposed by Belarbi and Hsu (1995) was used. To simulate the inelastic behavior of the concrete, the concrete damaged plasticity model (ABAQUS 2010) was used with 31 degree of the dilation angle. In the case of the steel, two different material properties were considered. For the first steel model, the yield and ultimate stress of the flange were set as 823.1 MPa and 920.8 MPa, respectively. In the case of the web, the yield and ultimate stress were 725.3 MPa and 867.3 MPa, respectively, based on the material test for the steel shown in section 3.1. Second model was based on the nominal strength provided by the manufacture, where the yield and ultimate stress of the steel were 690 MPa and 800 MPa, respectively. For the reinforcing bar, average stress-strain relationship of the embedded reinforcing bar suggested by Belarbi and Hsu (1995) was used to simulate the material model of the reinforcing bar where yield stress of the reinforcing bar was taken as 400 MPa. In the case of the interface between reinforcing bar and concrete, it is assumed that the reinforcing bar and concrete was perfectly bonded by using EMBEDED option in

ABAUQS (2010). The concrete slab and the girder were also perfectly bonded by using the TIE option in ABAQUS (2010), since full shear connector was assumed in this study.

4.2 Parametric study and discussion of analysis results

A total number of 13 models were constructed for the parametric study. All analysis models were design to meet the slenderness limit for the flange, web, and unbraced length specified in AASHTO LRFD Appendix B6 (2007). It should be noted that AASHTO LRFD Appendix B6 (2007) specify the limit of the yield stress as 485 MPa. However, recent research shows that it is still valid for the high strength steel (Joo *et al*. 2013). The main parameters were flange slenderness ratio λ_f where $\lambda_f = b_f/(2t_f)$, web slenderness ratio λ_w where $\lambda_w = 2D_{cp}/t_w$, unbraced length slenderness ratio λ_L where $\lambda_L = L_b/\gamma_t$, and normalized unbraced length factor α. λ_f, λ_w, and λ_L were normalized by λ_{pf}, λ_{pw}, and λ_{pL}, respectively. λ_{pf}, λ_{pw}, and λ_{pL} are the slenderness limit for the flange, web, and unbraced length specified in AASHTO LRFD Appendix B6 (2007), respectively. The basic properties and the ranges of the main parameter of the analysis models are shown in Table 1.

The analysis results were compared with proposed equation in section 2.1 and the results of previous researchers (Chen and Jia 2007, Kemp 1996), as shown in Fig. 15. The *x* axis of the Figs. 15(a), (b), and (c) represent the predicted available rotation capacity from the proposed equation of this study, Chen and Jia (2007), and Kemp (1996), respectively. The *y* axis denotes the available rotation capacity obtained from the analysis. It can be found that proposed equation gave the reasonably conservative prediction of the available rotation capacity for all analyzed models, while

Table 1 Analysis models for parametric study

Model	Dimensions (mm)	Material model	λ_f/λ_{pf}	λ_w/λ_{pw}	λ_L/λ_{pL}	α	f_c' of concrete slab
Case1	b_f= 120, h = 320, b_s = 1,200, t_s = 120	f_y = 823.1 MPa (flange) f_u = 920.8 MPa (flange) f_y = 725.3 MPa (web) f_u = 867.3 MPa (web)	0.48-1.09	0.41-1.46	0.89-1.82	0.5, 0.75	32 MPa
Case2	b_f= 800, h = 2400, b_s = 12,000, t_s = 360	f_y = 690 MPa f_u = 800 MPa					

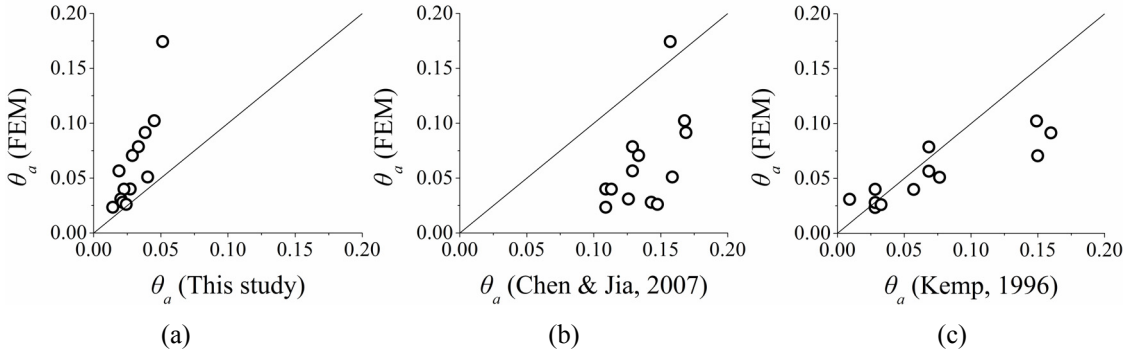

Fig. 15 Comparison of θ_a with analysis results: (a) this study; (b) Chen and Jia (2007); (c) Kemp (1996)

Chen and Jia (2007) gave an un-conservative prediction in most case. In the case of the equation proposed by Kemp (1996), it provide good estimation of the available rotation capacity when the available rotation capacity was smaller than 0.1. However, for the larger available rotation capacity, it gave un-conservative results. It might be attributed by the difference of material properties of the steel used for the derivation of the equations.

5. Conclusions

This study investigated moment redistribution of the continuous composite I-girder with high strength steel. Firstly, the available rotation capacity of the continuous composite I-girder with high strength steel was suggested based on the curvature distribution diagram (Eq. (1)). Then, the concept of the required rotation capacity of the continuous composite I-girder was presented. As an example, the required rotation capacity and failure load of the two-span continuous composite I-girder with uniform cross section and concentrated loads were proposed (Eqs. (6)-(8)).

A large scale test was conducted to examine the validation of the proposed equations. From the test results, it was found that the failure load and the required rotation capacity of the test specimens agree well with those from the proposed equations, and the proposed equations were successfully verified. However, it was hard to quantify the available rotation capacity of the continuous composite I-girder with high strength steel from the test result. Thus, additional verification was performed by using the non-linear finite element analysis. Based on the analysis results, it was found that the proposed available rotation capacity gave a reasonably conservative prediction of the available rotation capacity of the continuous composite I-girder with high strength steel.

Acknowledgments

The authors wish to acknowledge the financial support by Korea University and the Ministry of Land, transport and Maritime Affair (MLTM) through the Super Long Span Bridge R&D center in Korea. Also, this research was supported by a grant from R&D Program of the Korea Railroad Research Institute, Republic of Korea.

References

ABAQUS (2010), Abaqus Analysis User's Manual version 6.10, Dassault Systèmes Simulia Corp.

American Association of State Highway and Transportation Officials (AASHTO) (2007), LRFD Bridge Design Specifications, (4th Edition).

Barth, K.E., White, D.W. and Bobb, B.M. (2007), "Negative bending resistance of HPS70W girders", *J Construct. Steel Res.*, **53**(1), 1-31.

Belarbi, A. and Hsu, T.T.C. (1995), "Constitutive laws of softened concrete in biaxial tension-compression", *ACI Struct. J.*, **92**(5), 562-573.

Cevik, A. (2007), "Genetic programming based formulation of rotation capacity of wide flange beams", *J. Construct. Steel Res.*, **63**(7), 884-893.

Cevik, A. (2011), "Neuro-fuzzy modeling of rotation capacity of wide flange beams", *Expert Syst. Applicat.*, **38**(5), 5650-5661.

Chen, S. and Jia, Y. (2008), "Required and available moment redistribution of continuous steel-concrete

composite beams", *J Construct Steel Res*., **64**(2), 167-175.
Earls, C.J. and Shah, B.J. (2002), "High performance steel bridge girder compactness", *J. Construct. Steel Res*., **58**(5-8), 859-880.
Felkel, J.P., Rizos, D.C. and Ziehl, P.H. (2007), "Structural performance and design evaluation of HPS 70W bridge girders", *J. Construct. Steel Res*., **63**(7), 909-921.
Green, P.S., Sause, R. and Ricles, J.M. (2002), "Strength and ductility of HPS flexural members", *J. Construct. Steel Res*., **58**(5-8), 907-941.
Guzelbey, I.H., Cevik, A. and Gogus, M.T. (2006), "Prediction of rotation capacity of wide flange beams using neural networks", *J. Construct. Steel Res*., **62**(10), 950-961.
Joo, H.S., Moon, J. Choi, B.H. and Lee, H.E. (2013), "Rotation capacity and optimum bracing point of high strength steel I-girders", *J. Construct. Steel Res*., **88**, 79-89.
Kang, S.C., Kim, K.S. and Lee, J.K. (2011), "The evaluation of residual stresses in butt welded and fillet welded specimens with HSB800", RIST Research Paper, **25**(1), 1-7. [In Korean]
Kemp, A.R. (1996), "Inelastic local and lateral buckling in design codes", *J. Struct. Eng*., **122**(4), 374-382.
Kemp, A.R. and Dekker, N.W. (1991), "Available rotation capacity in steel and composite beams", *The Struct. Eng*., **69**(5), 88-97.
Kemp, A.R. and Nethercot, D.A. (2001), "Required and available rotations in continuous composite beams with semi-rigid connections", *J. Construct. Steel Res*., **57**(4), 375-400.
Lay, M.G. and Galambos, T.V. (1967), "Inelastic beams under moment gradient", *J. Struct. Div*., *ASCE*, **93**(1), 381-399.
Nie, J. and Cai, C.S. (2003), "Steel-concrete composite beams considering shear slip effects", *J. Struct. Eng*., **129**(4), 495-506.
Ricles, J.M., Sause, R. and Green, P.S. (1998), "High-strength steel: implications of material and geometric characteristics on inelastic flexural behavior", *Eng. Struct*., **20**(4-6), 323-335.
Sause, R. and Fahnestock, L.A. (2001), "Strengh and ductility of HPS-100W I-girders in negative flexure", *J. Bridge Eng*., **6**(5), 316-323.

CC